Journal of Structural Geology, Vol. 12, No. 3, pp. 383 to 395, 1990
Printed in Great Britain

0191-8141/90 $03.00+0.00

The Mohr diagram for three-dimensional reciprocal stretch vs rotation

SUSAN H. TREAGUS

Department of Geology, University of Manchester, Manchester M13 9PL, U.K.

(*Received* 20 *April* 1989; *accepted in revised form* 13 *October* 1989)

Abstract—Mohr diagrams for stretch provide a useful alternative to the more familiar λ',γ' Mohr diagrams, for solving two- and three-dimensional strain problems. Examples show how the polar graphs of stretch or reciprocal stretch vs rotation can be used to deform or undeform planes in three-dimensional strain. The strain ellipsoid can be represented by a three-circle reciprocal stretch diagram which represents the symmetric three-dimensional reciprocal stretch tensor. The diagram can also be applied to the representation of asymmetric three-dimensional deformation tensors. An example is given for a simple-shear deformation, which is represented by a distinctive 'off-axis' type of three-dimensional reciprocal stretch diagram.

INTRODUCTION

THE Mohr diagram for strain most widely used in structural geology is the Mohr circle for reciprocal quadratic elongation (λ') and unit shear (γ') (*sensu* Nadai 1950). Such Mohr circles appear in most text-books, as a graphical illustration of strain ellipse equations and as a method of determining a strain ellipse from a particular set of strain data. The popularity of the λ',γ' Mohr circle lies in its simplicity and its practical uses, as exemplified recently by Lisle & Ragan (1988).

An alternative Mohr circle for finite strain is the Mohr circle for the *stretch tensor* (Choi & Hsü 1971, De Paor 1981, 1983, Means 1982, 1983, De Paor & Means 1984). All Mohr circles are representations of rank-2 tensors (see De Paor & Means 1984); the stretch tensor (like the stress tensor represented by a Mohr stress circle in σ,τ space), is a physically more meaningful tensor than the reciprocal quadratic elongation (quadratic stretch) tensor. Moreover, the Mohr circle for stretch provides a method not only to represent the symmetric stretch tensor, **S**, but also the asymmetric *deformation tensor*, **D** (i.e. *position gradients tensor*). De Paor (1983), Means (1983) and De Paor & Means (1984) have shown that the Mohr representation of **D** can be an *off-axis Mohr circle*; an on-axis stretch circle is moved 'off' the graph axis (abscissa) by the rigid rotation component, the *rotation tensor*, **R** (Means 1983, fig. 3b) (see, also, Lister & Williams 1983, Bobyarchick 1986, Passchier 1988a,b). These authors demonstrate how such Mohr circles can be used to illustrate tensor operations, and how stretches, strains and rotations interact to produce deformation, in two dimensions.

The Mohr stretch circle is relatively new to structural geology, and has not had time to achieve the text-book coverage given to the λ',γ' circle. Its use to illustrate tensor operations may have disguised its simplicity as a graph for illustrating two-dimensional strain. Personal communications with D. G. De Paor and W. D. Means (1987–1988) have demonstrated to me the advantages of using the stretch circle rather than the 'familiar' λ',γ' Mohr circle for solving some two-dimensional problems, for illustrating forward and backward deformation, and for comparing pure and simple shear deformation. Recently, Passchier (1988a) and Passchier & Urai (1988) have illustrated how such Mohr circles might be applied to certain natural deformation structures.

One problem remains with the Mohr circle: it only represents two-dimensional stretch or deformation. (This is true for all Mohr circles; for example the comparable velocity gradients Mohr circle, $\dot{e},\dot{\omega}$—Means 1983, Lister & Williams 1983, Bobyarchick 1986, Passchier 1988a—is also only two-dimensional). Yet geological deformations cannot be considered as entirely two-dimensional, even plane strains. The rank-2 deformation tensors represented on Mohr circles by De Paor and Means are simply one principal plane of deformation, the maximum–minimum plane. Their discussions of deformation and illustrations of how the component tensors are multiplied (De Paor & Means 1984) are, by definition, restricted to this one plane of consideration. However, all planes in a three-dimensional deformation can be represented by a Mohr stretch circle, just as a λ',γ' circle can be derived for any strain ellipse (not usually a principal section). Whether such general Mohr stretch circles are on or off axis (i.e. fixed or rotated principal axes) will depend on what is taken as the 'fixed' frame from which to measure rotation.

The topic of this paper is to investigate some applications of the stretch diagram for three-dimensional strain. This will be called the *Mohr stretch diagram*, because it consists of more than one circle. It is analogous to the λ',γ' three-circle Mohr diagram for three-dimensional strain introduced by Nadai (1950, p. 129), applied to geological strain problems by Brace (1961) and Ramsay (1967, p. 170), and reviewed by Treagus (1986). Treagus presented a method of representing sectional strain ellipses on the λ',γ' Mohr diagram. The present account brings these same principles to the

three-circle Mohr diagram for stretches and rotations in three dimensions, in order to investigate its potential use for solving three-dimensional strain problems.

MOHR CIRCLES FOR STRETCH IN TWO DIMENSIONS

Stretch can be represented on Mohr circles of two types (De Paor 1981, Means 1982). One is for the *stretch tensor*, S, with angles measured in the undeformed state, and the other for the *reciprocal stretch tensor*, S', with angles measured in the deformed state (Fig. 1). These two circles are equivalent to the two quadratic stretch ellipses/circles (λ,γ and λ',γ') (Nadai 1950, Brace 1961). The difference between the stretch and quadratic stretch circles lies in the graph co-ordinates. The familiar λ',γ' circle is a Cartesian graph with abscissa, λ', and ordinate, γ'. The Means and De Paor stretch circles are *polar graphs*, with all values of S or S' in the strain ellipse measured radially from the graph origin, and all rotations of lines in the ellipse (ω) given by the ray inclination.

Figure 1 shows the two types of stretch circle (after Means 1982, figs. 1 and 4) for a known strain ellipse (principal axes S_1, S_2), and arbitrary line L. For both circles, the rotations of particular lines (e.g. L–L') are the same. Only in the special case of unit-area plane strain have the two circles the same diameter and position, which can allow S and S' to be plotted together on the one figure (e.g. De Paor 1983, fig. 21b) (with care not to confuse sign conventions). In all other cases (e.g. Fig. 1), the two circles are different so it is prudent to concentrate on one or the other. The present paper will concentrate on the reciprocal stretch diagram, S', where angles are measured in the final state, as seen in deformed rocks. However, the principles are equally applicable to the stretch diagram, S.

THE PRINCIPAL MOHR CIRCLES FOR STRETCH

A strain ellipsoid contains three principal strain ellipses, each of which may be represented by a Mohr stretch circle (Fig. 2); these may be called the *principal Mohr circles*. Together, these three circles define a *Mohr stretch diagram*, where all stretches and rotations for the strain ellipsoid fall in the shaded field bounded by the three circles (Fig. 2). A distinction must now be made between rotation angles, ω, measured in two dimensions on a single Mohr circle, and angular rotations in three dimensions, here termed ρ, measured on a full three-circle Mohr stretch diagram. For two-dimensional rotations, $\omega = 0$ will denote the strain ellipse axes (regardless of whether these have themselves rotated in three dimensions), and for three-dimensional rotations, $\rho = 0$ will denote the ellipsoid axes. The distinction between two- and three-dimensional rotations are analogous to the two- and three-dimensional shear strain components, $\gamma'_{\|}$ and γ'_{T} on the λ',γ' diagram of Treagus (1986).

The three principal Mohr circles can provide a simple method of determining rotations of oblique planes in a strain ellipsoid, by making use of their principal-plane

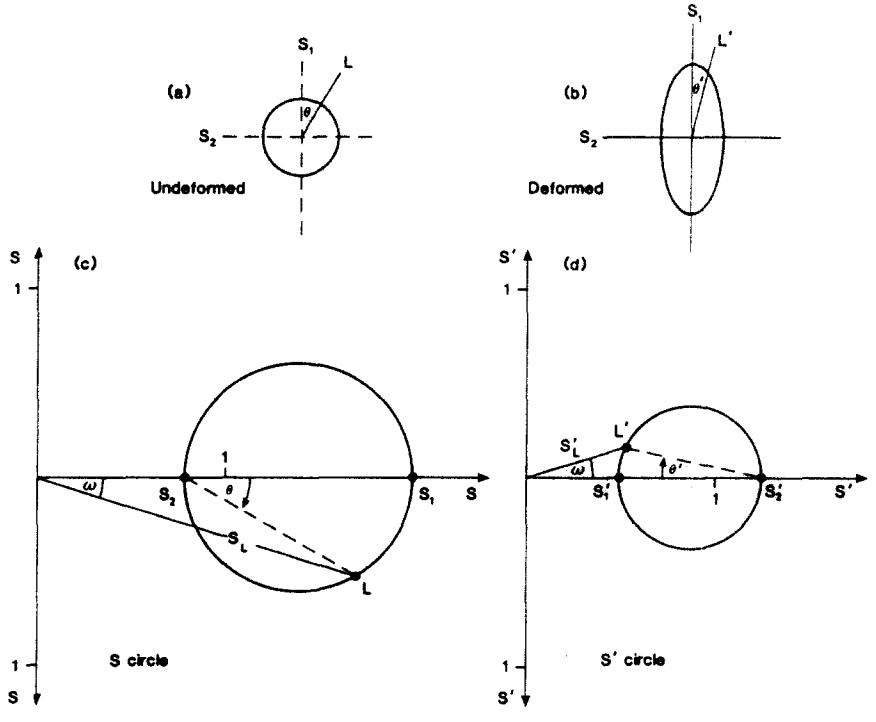

Fig. 1. The two types of Mohr stretch circle, after Means (1982). (a) Initial undeformed state (circle) with initial principal stretch axes, S_1, S_2, and arbitrary line ($\theta = 30°$). (b) Strain ellipse; $S_1 = 2$, $S_2 = 0.8$. (c) Mohr stretch circle, (S, ω) for the undeformed state. (d) Mohr reciprocal stretch circle, (S', ω) for the deformed state. $S'_1 = 0.5$, $S'_2 = 1.25$, $\theta' = 13°$. ω for L and L' is 17°. Both Mohr circles represent angles (θ, θ') in their true sense, so are of the "first kind" (De Paor & Means 1984).

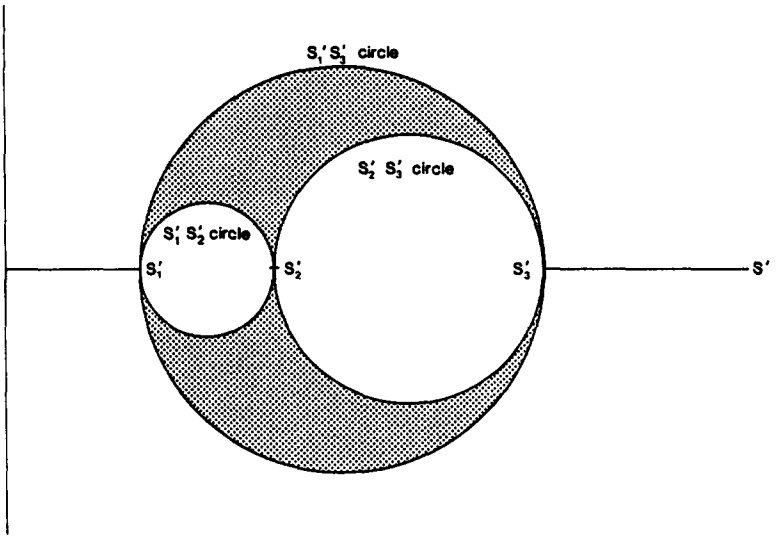

Fig. 2. The three principal reciprocal Mohr stretch circles. The three circles bound the region (shaded) of reciprocal stretches and angular rotations in three dimensions, for the whole strain ellipsoid.

intersections. Figure 3(a) shows a general section plane of a strain ellipsoid which is not parallel to any principal axes, but crosses the principal planes on lines A', B', C'. Points A', B', C' can be plotted on the three principal Mohr stretch circles (Fig. 3b) in the same manner as any line of known orientation such as L' in Fig. 1(d). It is convenient, here, to use half-circle diagrams, as in Treagus (1986), because the diagram is mirrored across the abscissa. (The question of a sign convention for rotations in three dimensions will be addressed in a later section, where the non-mirrored off-axis diagram is introduced.) Note that the Mohr diagram in Fig. 3(b) only represents the three principal-plane intersections in the oblique plane, and does not illustrate stretches and rotations for other lines in the plane. How these points link up to illustrate the whole plane will be discussed in the next section.

The reciprocal stretches and angular rotations for lines A', B', C' can be read off from the three Mohr semi-circles in Fig. 3(b). Each line has its full rotation in the strain ellipsoid (ρ) defined by its position on the principal Mohr circle it lies on (since the principal planes have zero rotation). Therefore, the section plane can be restored to its original orientation (A, B, C) in the strain ellipsoid (Fig. 3c). (The same simple procedure can be applied to find the distorted position of a plane of known original orientation, using the S Mohr diagram.)

Now, it should be possible from the information in Figs. 3(a) & (b) (i.e. three stretches and their orientations) to determine the strain ellipse for this section plane, and represent it with a Mohr circle. The Mohr stretch circle will have the same S' ray values for A', B', C' as in Fig. 3(b), but now measures the rotations of A', B', C' *within* the plane (i.e. ω). The presently unknown strain ellipse axes will be points of zero ω.

A method of constructing the A', B', C' sectional ellipse Mohr circle (for reciprocal stretch) for the example in Fig. 3 is presented in Fig. 4. First, measure $\angle$AB, $\angle$BC and $\angle CA$ in the plane, before and after deformation (angles shown in Figs. 3a & c), and sketch the original and deformed triangles (Figs. 4a & b). Choosing two lines (e.g. A, B), measure the difference in $\angle AB$ in the plane, before and after deformation, which is their *differential rotation*, Δ (66° − 55° = 11°). Then trace the three reciprocal stretch arcs for A', B', C' from the principal Mohr circles in Fig. 3(b) (Fig. 4c). Define an arbitrary point for A' on the A' arc, and draw its ray from the origin. Then draw the B' ray inclined at Δ to it. (There are two senses possible for Δ, but only one will allow a circle to be constructed.) Where the B' ray crosses the B' arc is point B'. Join A' and B' (Fig. 4c). The $A'B'C'$ triangle (similar to Fig. 4a) can now be drawn (Fig. 4d) and the Mohr circle constructed to fit this triangle. It may be noted that this construction has some similarities to Ramsay's (1967, pp. 130–134) triangular constructions to determine angular shear, but in the present case, the triangle angles are measured from Fig. 3(a), not constructed. Lisle & Ragan (1988) present a simpler method for constructing a λ',γ' Mohr circle to solve the 'three-stretch problem' graphically, but this does not work analogously on the polar stretch diagram.

An alternative method of determining a sectional Mohr stretch circle from a Mohr diagram for a strain ellipsoid would be to use the concept of a *Mohr locus* for stretch, analogous to that described by Treagus (1986) for λ',γ'. This is described below.

MOHR DIAGRAMS FOR STRETCH ELLIPSOIDS

The Mohr diagram for reciprocal stretch vs rotation in three dimensions is a *three-circle Mohr diagram* (Fig. 2) with identical geometry to that for three-dimensional stress (Mohr 1882) and reciprocal quadratic elongation (Nadai 1950, p. 129). The reciprocal stretch and rotation of any direction in a strain ellipsoid can be determined by construction, using its angles ϕ'_1, ϕ'_2, ϕ'_3 to principal stretch axes (Fig. 5), as already described for other Mohr

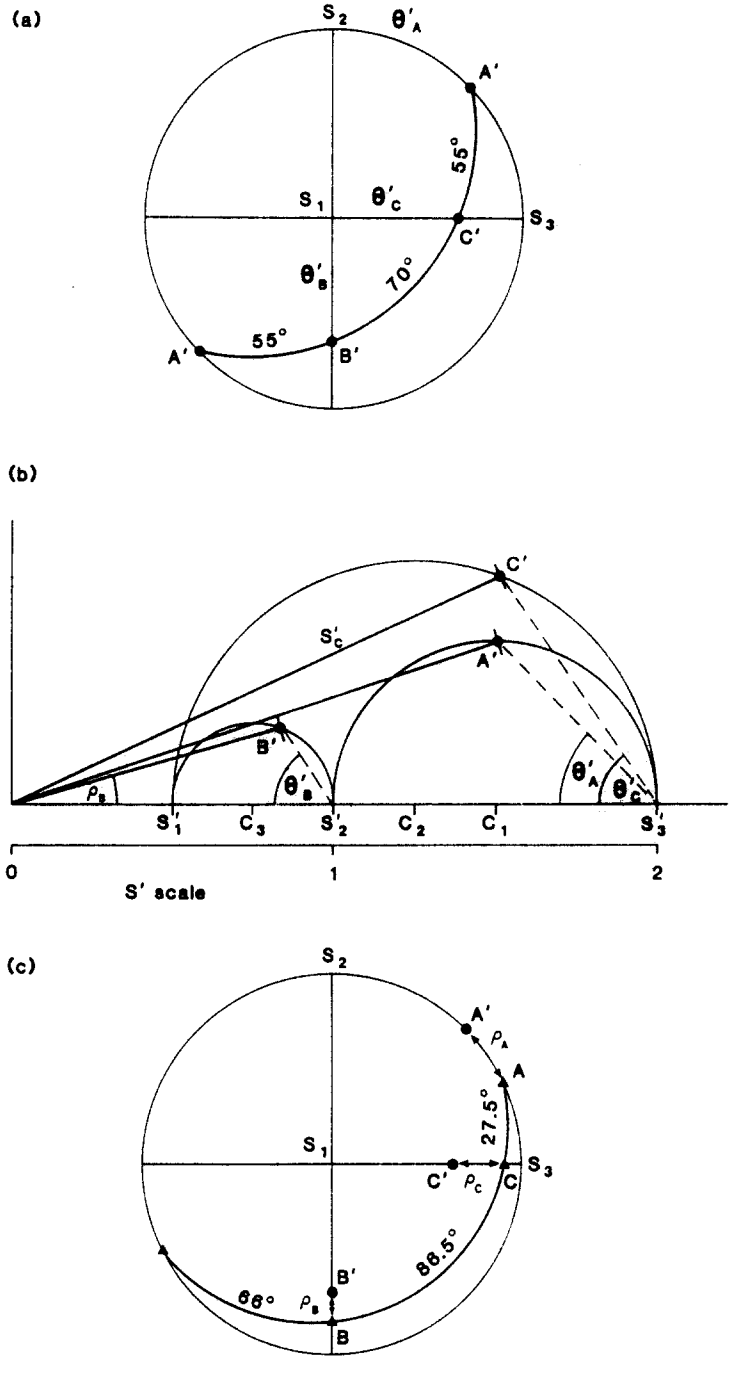

Fig. 3. Example of the construction of the rotation of an oblique plane in a known strain ellipsoid. (a) An oblique plane, 045°/45°SE. A', B' and C' are the principal-plane intersections, and $\theta'_A = 45°$, $\theta'_B = 55°$, $\theta'_C = 55°$. (b) Construct A', B' and C' on the three principal half Mohr circles, using the three θ' angles. Measure the rotation angles (e.g. ρ_B) for A', B', C'. ($\rho_A = 19°$, $\rho_B = 16°$, $\rho_C = 25°$.) (c) Restore A', B', C' to their original positions, A, B, C, on the principal planes, using these ρ values (e.g. $\theta_A = \theta'_A + \rho_A$). This determines the initial position of the section plane: $\theta_A = 54°$, $\theta_B = 71°$, $\theta_C = 80°$. Angles AB, BC and AC are measured and labelled, for use in Fig. 4(b). (a) and (c) are lower-hemisphere, equal-area projections.

diagrams (e.g. Ramsay 1967, pp. 147–153, Treagus 1986, figs. 1 and 3). However, recall that unlike the σ, τ or λ',γ' Cartesian graphs, the Mohr stretch diagrams use polar co-ordinates. In Fig. 5(b), the reciprocal stretch of L' (S'_L) is its radial distance from the origin, and its *total rotation in three-dimensional strain* (with respect to fixed ellipsoid axes) is angle ρ_L. Recall that the line L' in Fig. 5 may be contained on any number of sectional ellipses, whose particular Mohr circles only record the proportion of ρ in the plane of section (denoted ω). An understanding of the difference between two-dimensional (ω) and three-dimensional rotations (ρ), like the difference between two- and three-dimensional shear strain discussed in Treagus (1986), is fundamental to the jump from two- to three-dimensional strain analysis.

A Mohr diagram does not provide the *direction* of shear stress or strain, nor in the present case, directions of three-dimensional rotation (ρ_L); a secondary construction is required, following the Zizicas (1955) con-

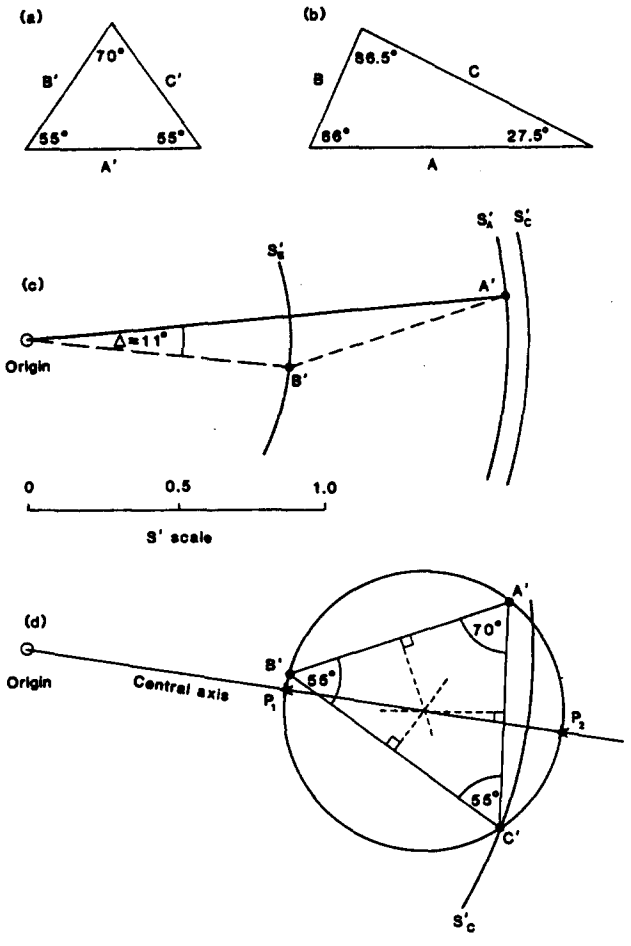

Fig. 4. Determination of the strain ellipse for the section plane in Fig. 3. (a) and (b) show the on-plane positions of A, B, and C, after and before straining, respectively. The relative rotation of B to A (Δ) is 11°. (c) Draw the reciprocal stretch arcs for A', B', B', using ray values in Fig. 3(b). Draw an arbitrary ray to locate A'. Draw another ray at angle Δ to the A' ray; where it crosses the S'_B arc is point B'. Join A' and B'. (d) Draw a triangle on $A'B'$ 'similar' to triangle (b), to locate C'. Construct a circle to fit this triangle, which is the Mohr circle (reciprocal stretch) for the section plane. The line from the origin through the circle centre defines the graph abscissa (not horizontal in this example). The principal axes lie on the abscissa. Result: reciprocal principal stretches 0.86 (P_1) and 1.77 (P_2); P_1 at ≈3° to B'.

struction for stress (see, also, Jaeger & Cook 1969, p. 30, Johnson & Mellor 1973, p. 52). Since all Mohr diagrams are topologically equivalent, the Zizicas construction can be applied equally well to the stretch diagram. The method depends on the fact that a section which contains L' and one principal ellipsoid axis can be constructed as a circular arc. This introduces the general concept of representing sectional ellipses as *Mohr loci* on the stretch diagram.

Sectional ellipse loci

The types and shapes of sectional ellipses on the Mohr stretch diagram are identical to those described for the λ',γ' diagram in Treagus (1986). Sectional ellipses can be classified into three types, which are illustrated in Fig. 6.

(1) Principal sections of ellipsoids are whole circles, or semi-circles if rotation direction (sign) is neglected (Fig. 6a). In this paper, these are called the principal Mohr circles.

(2) Sections containing one principal stretch axis are circular arcs passing through the particular principal axis, with centres on the graph abscissa (see Treagus 1986, fig. 6). One example from each of the three sets of planes is shown in Fig. 6 (b, i–iii). This type of section is used in the Zizicas construction, as described below.

(3) Generally oblique sectional ellipses are represented by loops on the half Mohr diagram (e.g. Fig. 6c). More examples of locus shapes are shown in Appendix Fig. A1 (see also Treagus 1986, fig. 8). These loci will be investigated later.

To determine directions of three-dimensional rotation

Consider the general line, L' in Fig. 5, and its three-dimensional rotational angle, ρ_L. Following the Zizicas construction (1955), draw a plane through one principal axis and L'; the S_1 axis is used here (Fig. 7a). Construct the Mohr locus of this plane (Fig. 7b); it is a type-2 locus,

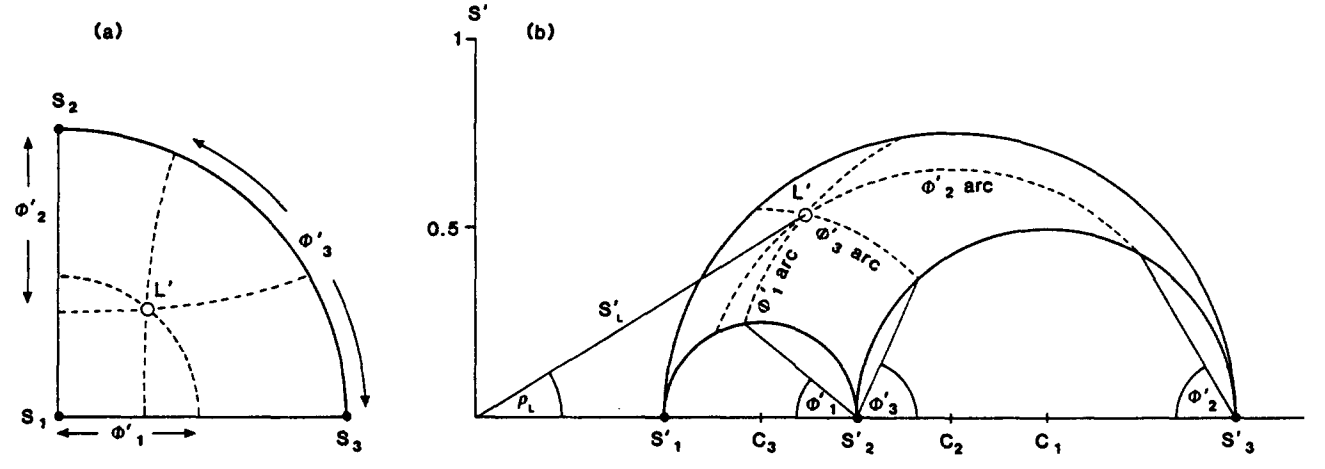

Fig. 5. The location of an arbitrary line L' on a Mohr diagram, using ϕ'_i angles ($\phi'_1 = 40°$, $\phi'_2 = 60°$, $\phi'_3 = 66.5°$). (a) A quadrant lower-hemisphere, equal-area projection defining the ϕ'_i small circles to S_i. (b) The ϕ'_i small circles are circular arcs on the Mohr diagram; ϕ'_1 is concentric with the $S'_2S'_3$ circle, centre C_1, and so on. The S'_L, ρ_L values are easily read off (1.02, 32°).

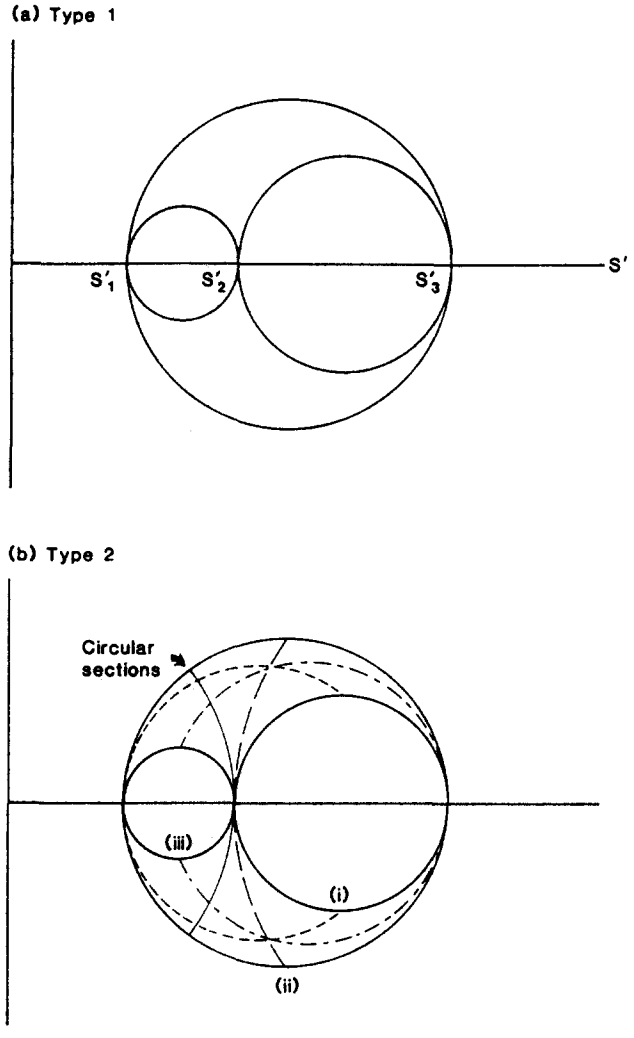

Fig. 6. Classification of sectional ellipse Mohr loci. (a) Type-1 are the principal planes, which are full circles. (b) Type-2 are planes containing one principal axis, which are partial circles centred on the abscissa. Four planes are shown. Solid curve: circular section ($S' = S'_2$). Short-dash curve (i): plane parallel to S'_1 and 45° to S'_2 and S'_3. Long-dash curve (ii): plane parallel to S'_2 and 45° to S'_1 and S'_3. Dot-dash curve (iii): plane parallel to S'_3 and 45° to S'_1 and S'_2. For each, the arc centre is given by the intersection of the perpendicular bisector of the line joining the particular principal axis (e.g. S'_3) to the 45° point on the principal circle (S'_1, S'_2). (See also Fig. 7b.) (c) Type-3 loci are planes oblique to all three principal axes. The example is plane 045°/45° from Fig. A1 (also Fig. 3). It is a loop which is tangential to the principal circles at A', B', C', its principal-plane intersections.

a circular arc centred on the abscissa (see Fig. 6b). Label point T' its intersection with the $S'_2S'_3$ circle. The rotation of point T is ρ_T. The principal ellipse axes for the S_1–L'–T' plane are the minimum and maximum S' values, which are S'_1 and T'. A Mohr circle is drawn with these values (Fig. 7c). Now draw an arc from the graph origin through L' which 'swings' L' from the three-dimensional Mohr diagram (Fig. 7b) to the two-dimensional Mohr circle ($\underline{L}'$, Fig. 7c). The angle ϕ'_1 of L' to S_1 is now measured on the circle, and can be checked with Fig. 7(a). Measure the rotation of $\underline{L}'$ on the Mohr circle (ω_L, Fig. 7c); this is $(\phi_1 - \phi'_1)$.

The relationship between the three angles, ρ_L, ω_L and ρ_T are shown in Fig. 7(d). The *direction* of rotation of line L with respect to the principal stretch axes is shown by the solid arrow. The same result would be obtained by using planes through S_2 or S_3, but these are slightly less convenient than the straight-line plane on the stereographic orientation used here. This Zizicas construction is one of many possible constructions for determining rotation sense by splitting the three-dimensional rotation into two-dimensional components (compare with the γ' method in Treagus 1986).

Figure 7 serves to illustrate the relationship between rotations in three dimensions (in the ellipsoid) and in two dimensions (within the section plane) for a type-2 Mohr locus. The next section will examine this relationship for more general type-3 Mohr loci.

MOHR LOCI FOR OBLIQUE SECTIONAL STRETCH ELLIPSES (TYPE-3)

General sections of strain ellipsoids which are oblique to all three axes are represented on Mohr diagrams by variably shaped arcuate loops (Figs. 6c and A1). These type-3 Mohr loci cannot be easily predicted, nor constructed exactly, from just two or three points (see Treagus 1986). For example, the points A', B', C' on Fig. 3(b) could be fitted to a circle, triangle, ellipse, etc. The graphical method used in Treagus (1986, fig. 6) relied on beginning by plotting the principal-plane intersections (A', B', C'), adding the circular-plane intersections, and then choosing a few more points on the section plane which required plotting according to their ϕ'_1, ϕ'_2, ϕ'_3 angles (defined in Fig. 5). This is somewhat tedious and inexact. In the Appendix, an algorithm is presented which can be used in a simple computer program to plot Mohr loci for planes (represented by an array of lines) in terms of their 'strike' and 'dip' to the principal stretch axes (S_1 vertical, S_2 N–S and S_3 E–W). The examples (Fig. A1) show that the shapes are variably arcuate, but not circular arcs.

For the λ',γ' loci for sectional ellipses shown in Treagus (1986), the principal ellipse axes (P_1, P_2) are the most extreme left and extreme right values of λ' (Fig. 8a). Exactly the same locus represents a sectional ellipse on the stretch diagram (Fig. 8b), but for a *different ellipsoid*, because the abscissa scale (for measuring principal axial values) is now reciprocal stretch rather than

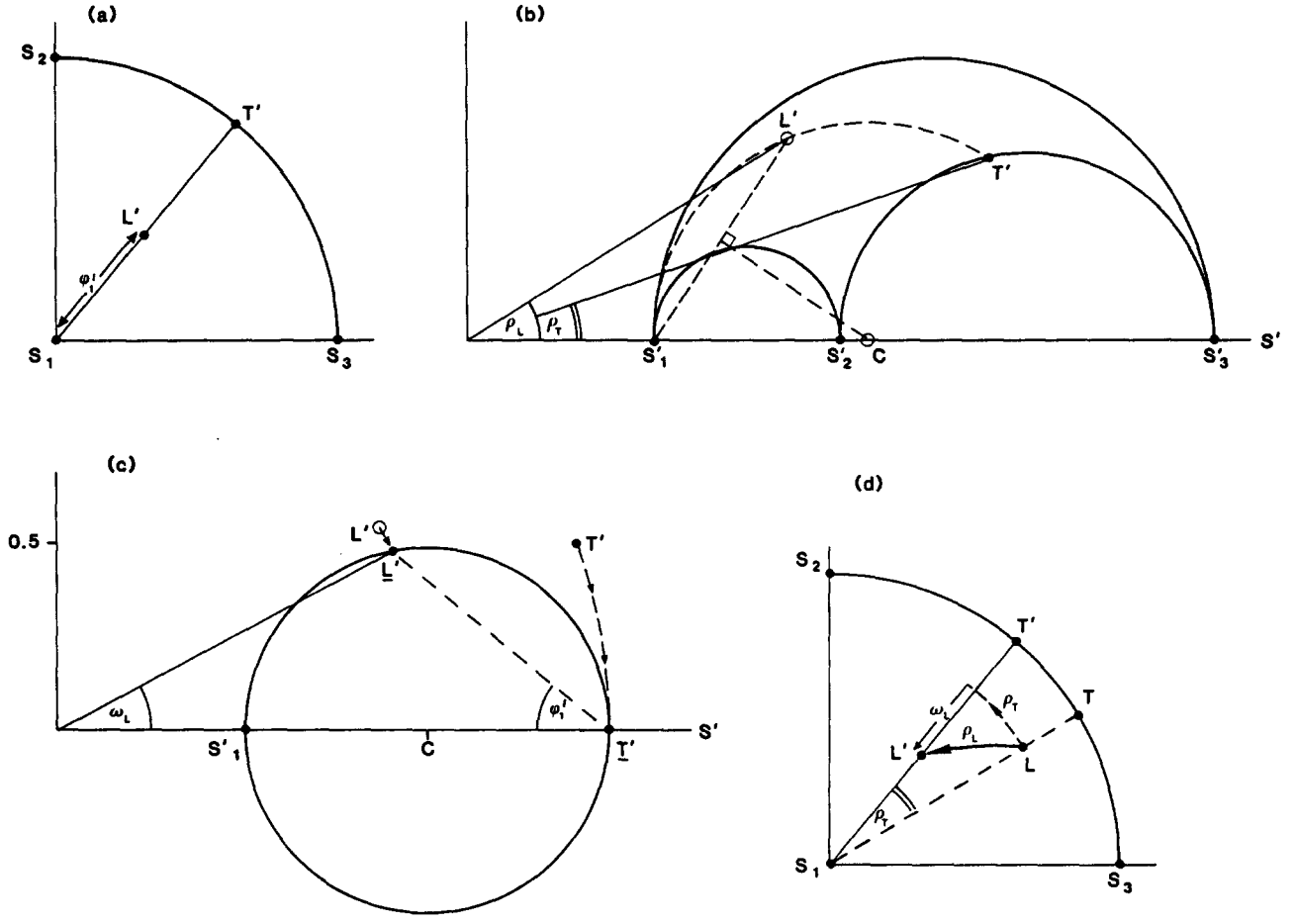

Fig. 7. Determination of the direction of rotation of an arbitrary line (L') in the strain ellipsoid, using a modified construction of Zizicas (1955). (a) Quarter stereographic representation locating L' (same L' as in Fig. 5a; $\phi'_i = 40°$). Draw a plane through S_1 and L' and label T' as shown. (b) Draw the half Mohr diagram and plot L', as in Fig. 5(b). ($\rho_L = 32°$.) Construct the circular type-2 Mohr locus (see Fig. 6b) for the S'_1L' plane by drawing a circular arc through S'_1, L', centred on the abscissa (C). Its intersection with the $S'_2S'_3$ circle locates T'. Measure ρ_T (19°). (c) Construct the Mohr circle for the $S'_1L'T'$ plane, on axes S'_1 and S'_T. Positions of L' and T' swung onto the Mohr circle are shown by underbars. Measure ω_L (28°), the component of rotation for L' in the plane of the Mohr circle. (d) The original position of L can be constructed, using three rotation angles: ρ_L is its total rotation; ρ_T is the total rotation of T', and thus the rotation of the S_1L' plane; ω_L is the component in the S'_1L' plane. The large arrow is the direction of rotation.

reciprocal quadratic stretch. For the reciprocal stretch locus (Fig. 8b), the principal ellipse stretch axes are given by the minimum and maximum *rays*. Thus, the Mohr circles in (a) and (b) are different, the former measuring λ',γ', and the latter S',ρ.

The above examples of stretches and rotations in three dimensions demonstrate three points about Mohr stretch diagrams and their sectional ellipse loci.

(1) On three-circle Mohr stretch diagrams, the total angular rotations (ρ) are recorded, relative to fixed ellipsoid axes. For type-3 loci, all lines of the section plane have rotated in the ellipsoid; there is no point of zero rotation.

(2) Any ellipsoid section plane can be represented by a Mohr stretch circle which only represents in-plane rotations (ω) relative to 'fixed' ellipse axes. However, for all general (type-3) sections, these ellipse axes have rotated in the ellipsoid.

(3) Neither the three-dimensional stretch diagram nor two-dimensional stretch circles record the three-dimensional deformation. The 'stretch + rotation' of general ellipse sections must therefore not be confused with the De Paor–Means off-axis Mohr circle for the two-dimensional deformation tensor, composed of a symmetric stretch tensor and a rigid rotation tensor within the *same* plane.

The last point introduces the idea of representing three-dimensional stretches and rotations for known deformations, which would be a three-dimensional version of the De Paor–Means representation of off-axis Mohr circles for rank-2 asymmetric deformation tensors.

OFF-AXIS MOHR DIAGRAMS FOR STRETCH AND ROTATION: THE THREE-DIMENSIONAL DEFORMATION TENSOR

All Mohr circles which represent two-dimensional stretch tensors will be, by definition, on-axis (Fig. 1), because stretch tensors are symmetric. In terms of the Mohr circle, this means that only rotations arising from two-dimensional strain are represented, and these are symmetrical about the strain ellipse axes. However, a

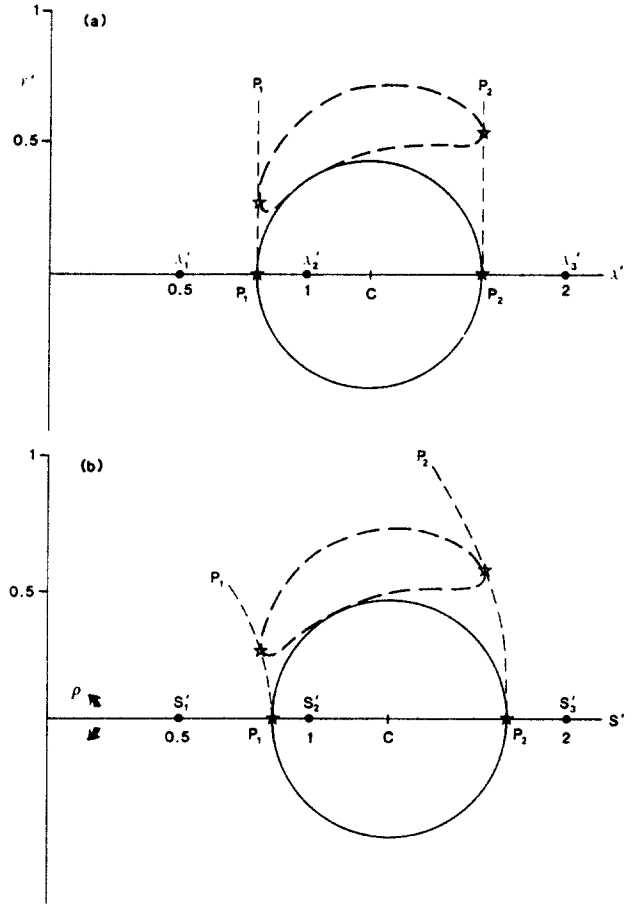

Fig. 8. The relationship between two identical type-3 Mohr loci (Fig. 6c) and their sectional ellipse Mohr circles, for two types of Mohr diagram. (a) the λ',γ' Mohr diagram, after Treagus (1986). Principal axes (P_1, P_2; starred) are the leftward and rightward points on the locus, which define the Mohr circle (0.81, 1.69). (b) The S',ρ diagram of this paper. P_1 and P_2 (starred) are defined on the locus by the minimum and maximum graph radii, which determine the diameter of the S', ω Mohr circle (0.86, 1.77) (as also derived in Fig. 4).

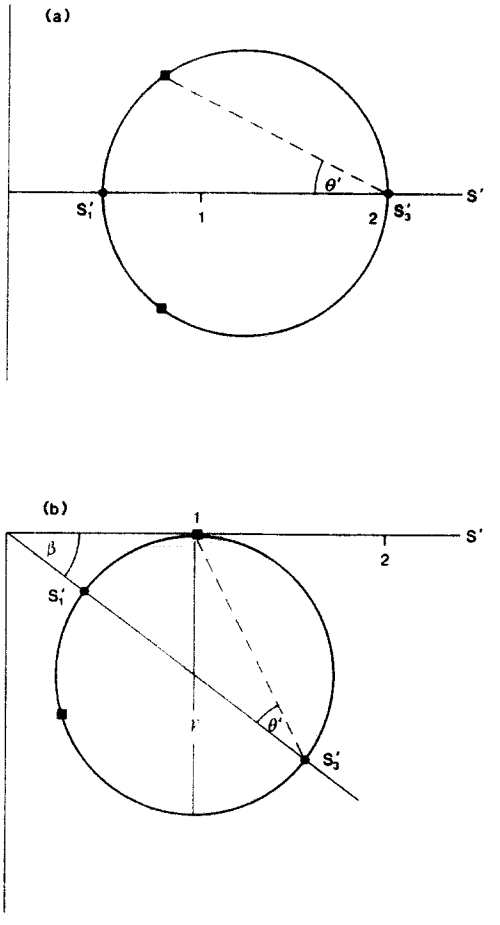

Fig. 9. 'On-axis' and 'off-axis' Mohr circles (S',ω) for two-dimensional deformation, after De Paor (1983) and Means (1983). (a) Pure shear (symmetric deformation tensor). Zero rotation of strain ellipse axes. (b) Simple shear (asymmetric) with shear strain γ (dextral). Rotation of ellipse axes by β ($=\tan^{-1}(\gamma/2)$). Both diagrams have the same strain ellipse. Squares show the lines of no finite longitudinal strain, at θ' to S_1' in each.

two-dimensional deformation involving strain *and* rotation of the strain axes has an asymmetric deformation tensor. This may be represented in Mohr-circle space by an off-axis Mohr circle, as introduced by De Paor (1981, 1983) and Means (1983). Figure 9 illustrates on- and off-axis Mohr circles (the "first kind" of De Paor & Means 1984) for two simple (two-dimensional) deformations: (a) pure shear and (b) simple shear. They have the same stretch tensor, **S**, shown by identical circles, but different deformation tensors, **D**, indicated by circle position, because of the different rigid rotation tensors, **R**. Pure-shear deformation is represented in two dimensions by a stretch circle centred on the abscissa (Fig. 9a) and simple-shear by a circle tangential to the abscissa (Fig. 9b), lying above for sinistral and below for dextral simple shear. The tangent point is the simple-shear direction, the only direction with zero rotation (the eigenvector).

Now consider Mohr diagrams for three-dimensional stretch and rotation, for pure-shear and simple-shear deformation. Clearly, the pure-shear diagram is the on-axis three-circle Mohr diagram already illustrated (Fig. 2), because the deformation tensor is the same as the stretch tensor (i.e. unit rotation tensor) (Fig. 10). It is appropriate, now, to use the full Mohr diagram rather than the half diagram, and devise a sign convention for three-dimensional rotations. The same convention can then be applied to Mohr diagrams which are not symmetric (i.e. off-axis). The signs chosen for rotations are defined in Fig. 10(b); the stereonet is divided into + (W) and − (E) 'sides', relative to viewing from the south. Use of the full Mohr diagram now changes the form of Mohr loci for sectional ellipses. The same looped locus shown earlier on the half diagram (Figs. 6c and 8b) is now split, and traverses the upper and lower Mohr vacancy field (Fig. 10c). Two sign changes occur at A' and B' as the plane crosses these principal planes, and 'jumps' across the appropriate Mohr circles.

The section plane shown in Fig. 10(d) (i.e. 045°/45°NW) is one of four geometrically equivalent planes in the ellipsoid. The plane mirrored on E–W (135°/45°SW) is also represented by the locus shown. The two planes mirrored on N–S (045°/45°SE and 135°/45°NE) have the reverse sign, and are thus represented by an upside-down form of Fig. 10(c).

Figure 11 is the equivalent Mohr stretch diagram to

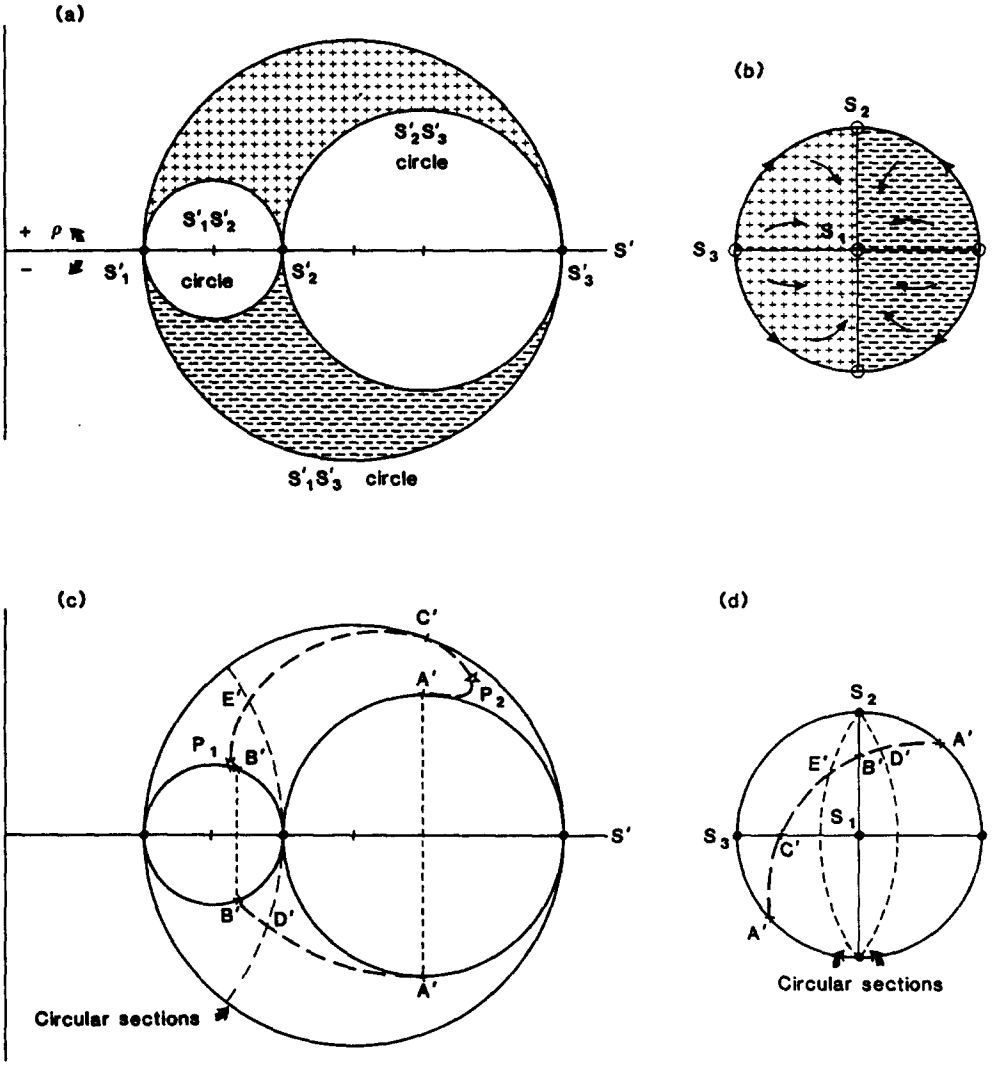

Fig. 10. The full three-dimensional Mohr diagram (S',ρ) for pure-shear deformation. (a) The three-circle diagram, showing the sign convention used. (b) Stereographic representation of the strain ellipsoid, showing the fields of + and − rotations and zero rotation (circles). (c) The Mohr locus for the oblique sectional ellipse example used previously (045°/45°; Figs. 6c, 8b and A1), represented stereographically in (d). Heavy broken curve is the sectional ellipse, with principal axes starred; solid curves are principal planes and fine broken curves circular sections. The pecked line indicates how the locus is split as it changes sign at A' and B'. An upside-down version of the locus in (c) represents the equivalent plane of reversed sign (see text).

Fig. 10, but for a simple-shear deformation. Both deformations have identical strain ellipsoids but different rigid rotation components. The Mohr diagram is a three-dimensional version of the off-axis Mohr circles of De Paor (1983) and Means (1983). The principal $S'_1S'_3$ plane is the De Paor–Means off-axis Mohr circle (e.g. Fig. 9b). However, the $S'_1S'_2$ and $S'_2S'_3$ principal planes are *not* full Mohr circles on the three-dimensional deformation diagram. They are represented by circular arcs, centred on the abscissa, which link the off-axis S'_1 or S'_3 points to the on-axis S'_2 point. These *principal Mohr arcs* are collapsed versions of the circles in Fig. 10, as they have no central vacancy. Similarly, one of the circular sections in Fig. 10 (i.e. the shear or flow plane) is collapsed to a single point in Fig. 11(a).

The full Mohr diagram for simple shear deformation is off-axis and asymmetric. Instead of lines or loci occupying the vacancies between the three principal circles (as shaded in Figs. 2 and 10a), here they occupy the whole region of the $S'_1S'_3$ circle. Figure 11(b) shows the rotation signs for simple shear, and it is clear that all rotations would be either positive (defined for sinistral simple shear) or negative (dextral, as here). The oblique-section plane shown in Figs. 11(c) & (d) has the same orientation in the ellipsoid as that in Figs. 10(c) & (d). Although the two Mohr loci appear very different in geometry, this difference is caused entirely by the different rigid rotation components. Equivalent lines on each locus have the same stretches. For both loci, the two-dimensional stretch is represented by the Mohr circle drawn in Fig. 8(b).

Mohr diagrams could be drawn for other three-dimensional deformations which are neither perfectly pure shear nor simple shear (three-dimensional equivalents of De Paor 1983, fig. 22; see also Bobyarchick 1986). The forms of these diagrams will be geometrically more complex than either Fig. 10 or Fig. 11, with a general trend of increasing asymmetry and complexity

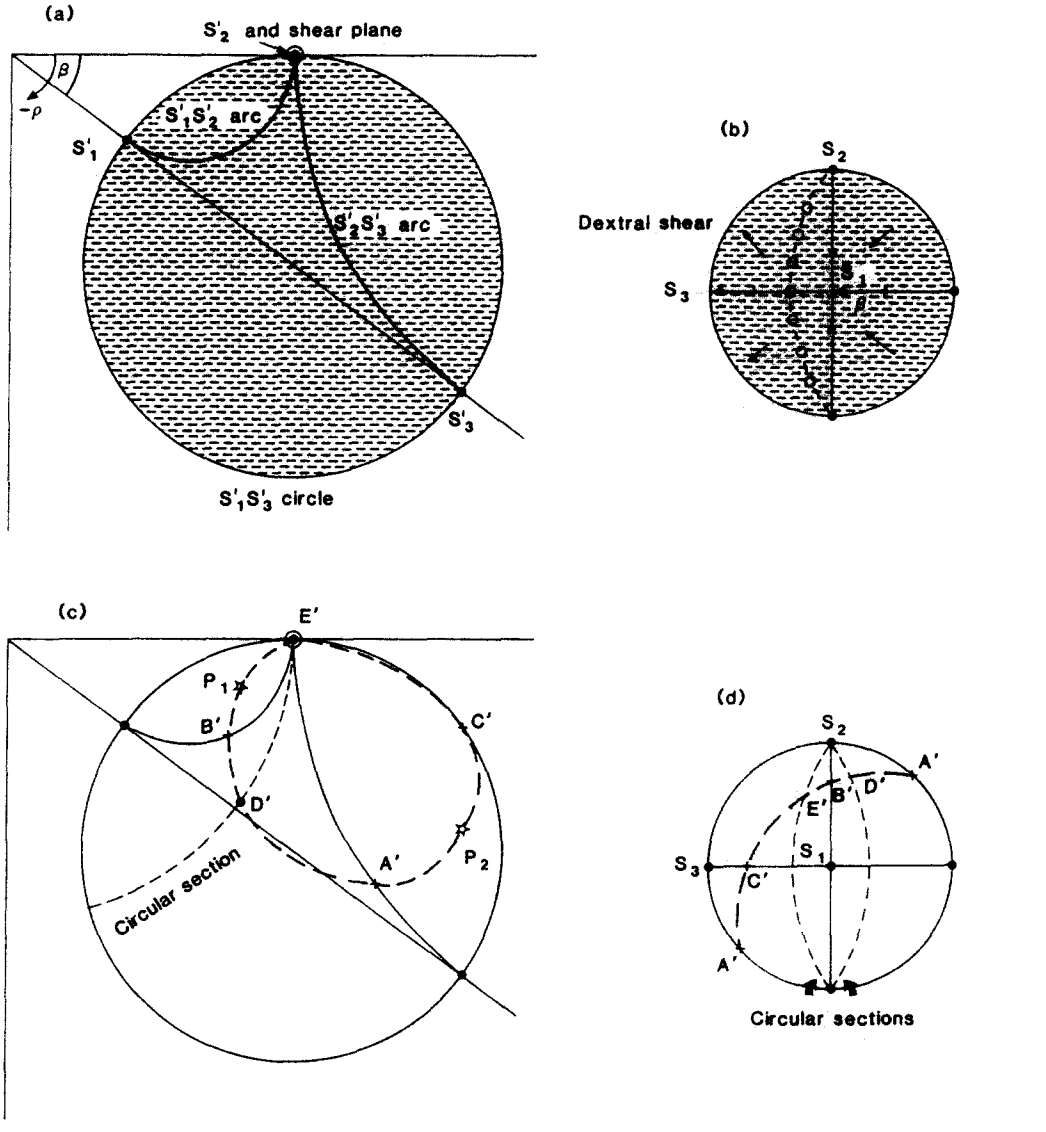

Fig. 11. The full three-dimensional Mohr diagram (S', ρ) for simple-shear deformation. The strain ellipsoid is the same as the pure-shear example in Fig. 10. Symbols as for Fig. 10. (a) The 'three-circle' diagram for dextral simple shear. All rotations are negative. See text for discussion of the features of this diagram. (b) Stereographic representation of the strain ellipsoid and rotations. All rotations are negative, except for the plane of shear (circles) which is zero. (c) Mohr locus for the oblique sectional ellipse example (see Fig. 10c). The locus, only constructed approximately here, is a continuous loop. It represents all four planes symmetrical in the ellipsoid to the plane shown stereographically in (d), unlike for pure shear. Note that the reciprocal stretches for A', B', C' and the principal ellipse axes, P_1 and P_2, in (c), are identical to those shown in Fig. 10(c).

with increasing rotational deformation. Lister & Williams (1983, fig. 3d) illustrated an analogous general three-dimensional flow on the $\dot{e},\dot{\omega}$ Mohr diagram, but this is an incorrect representation (G. S. Lister personal communication 1989). [On a Mohr diagram for three-dimensional flow, such a rotational flow should be represented by an even more off-axis diagram than the simple-shear example in Fig. 11, whereas the two-dimensional flow (Mohr circles) for the three non-principal planes in their fig. 3(d) would not be the tangential circles shown, but should intersect.]

These off-axis three-dimensional diagrams are not easy to understand or use. Even the simple-shear diagram is geometrically complex. Its only simple geometrical features are the circular arcs which represent principal planes and one circular section, and a single point for the shear-plane circular section (Fig. 11). Off-axis three-dimensional Mohr diagrams lack the following two features of the symmetric (on-axis) three-circle diagrams, which make them practicable.

(1) Small circles for ϕ'_1, ϕ'_2 and ϕ'_3 are circular arcs which segment the Mohr diagram (see Fig. 5). On the off-axis diagram these are no longer circles. Investigation of their form on the simple-shear diagram (Fig. 11) has yielded no predictable geometry for ϕ'_i small circles, which would allow points to be plotted easily on off-axis Mohr diagrams.

(2) Planes containing one principal axis are represented by circular arcs, centred on the abscissa (type-2 Mohr loci; Fig. 6b). This is fundamental to various constructions (e.g. Zizicas 1955). It is not found to be true for the simple-shear diagram (Fig. 11) and thus will not be true for any three-dimensional off-axis diagram.

As a consequence of the two points above, the off-axis

Mohr diagram is a difficult graph to use. Its main merit may be to demonstrate the complexities of rotations in three-dimensional deformation involving rotational strains.

CONCLUSIONS

The Mohr diagram for three-dimensional stretches and rotations provides a useful graphical method for restoring orientations of planes and lines in three-dimensional strain. Examples here have concentrated on the reciprocal stretch diagram which can be used to determine unknown original orientations from known principal strains and final orientations. However, the same principles can be applied to forward straining, using stretch values and original angles. Both the stretch and reciprocal stretch Mohr diagrams for three-dimensional strain are representations of the symmetric three-dimensional stretch tensor, so the diagrams are, by definition, mirrored across the abscissa. It is therefore a convenient simplification to disregard the sign of rotations in three dimensions, and use a half Mohr diagram for stretch.

The Mohr diagram for stretch and rotation can also be used to represent the three-dimensional deformation tensor, which is only symmetric in the case of irrotational deformation. The full, rather than half, Mohr diagram is now required. The diagram for simple-shear deformation in three dimensions illustrates the complexities of this simplest kind of off-axis Mohr diagram, as a representation of three-dimensional rotations and stretches. This serves as a reminder that two-dimensional analyses and Mohr circle illustrations do not adequately demonstrate the effects of three-dimensional deformation.

Acknowledgements—I should like to thank the Geology Department, University of Manchester, for providing facilities for this research. Particular thanks go to Nick Hill and Richard Mason for help in the computer plotting of Mohr loci, and to Richard Hartley for drawing the diagrams. This work was inspired by many personal communications with Win Means and Declan De Paor, who also suggested improvements to the paper. Cees Passchier, Donal Ragan and Dave Sanderson are thanked for their reviews which provided many ideas for further improvement.

REFERENCES

Bobyarchick, A. R. 1986. The eigenvalues of steady flow in Mohr space. *Tectonophysics* **122**, 35–51.

Brace, W. F. 1961. Mohr construction in the analysis of large geologic strain. *Bull. geol. Soc. Am.* **72**, 1059–1080.

Choi, C. Y. & Hsü, T. C. 1971. Mohr circles for large and small strains in two-dimensional deformations. *J. Strain Analysis* **6**, 62–69.

De Paor, D. G. 1981. Geological strain analysis. Unpublished Ph.D. thesis, National University of Ireland.

De Paor, D. G. 1983. Orthographic analysis of geological structures—I. Deformation theory. *J. Struct. Geol.* **5**, 255–277.

De Paor, D. G. & Means, W. D. 1984. Mohr circles of the First and Second Kind and their use to represent tensor operations. *J. Struct. Geol.* **6**, 693–701.

Jaeger, J. C. & Cook, N. G. W. 1969. *Fundamentals of Rock Mechanics*. Chapman & Hall, London.

Johnson, W. & Mellor, P. B. 1973. *Engineering Plasticity*. Van Nostrand Reinhold, London.

Lisle, R. J. & Ragan, D. M. 1988. Strain determination from three measured stretches—a simple Mohr circle solution. *J. Struct. Geol.* **10**, 905–906.

Lister, G. S. & Williams, P. F. 1983. The partitioning of deformation in flowing rock masses. *Tectonophysics* **92**, 1–33.

Means, W. D. 1982. An unfamiliar Mohr circle for finite strain. *Tectonophysics* **89**, T1–T6.

Means, W. D. 1983. Application of the Mohr-circle construction to problems of inhomogeneous deformation. *J. Struct. Geol.* **5**, 279–286.

Mohr, O. 1882. Ueber die Darstellung des Spannungszustandes und des Deformationszustandes einges Körperelementes und über die Anwendung derselben in der Festigkeitslehre. *Civilingenieur* **28**, 113–115.

Nadai, A. 1950. *Theory of Flow and Fracture of Solids*. McGraw-Hill, New York.

Passchier, C. W. 1988a. Analysis of deformation paths in shear zones. *Geol. Rdsch.* **77**, 309–318.

Passchier, C. W. 1988b. The use of Mohr circles to describe non-coaxial progressive deformation. *Tectonophysics* **149**, 323–338.

Passchier, C. W. & Urai, J. 1988. Vorticity and strain analysis using Mohr diagrams. *J. Struct. Geol.* **10**, 755–763.

Ramsay, J. G. 1967. *Folding and Fracturing of Rocks*. McGraw-Hill, New York.

Treagus, S. H. 1986. Some applications of the Mohr diagram for three-dimensional strain. *J. Struct. Geol.* **8**, 819–830.

Zizicas, G. A. 1955. Representation of three-dimensional stress distribution by Mohr circles. *J. appl. Mech.* **22**, 273–275.

APPENDIX

AN ALGORITHM FOR PLOTTING MOHR LOCI

The section plane is treated as an array of lines lying in the plane, which are then plotted as a series of points on a Mohr diagram. The algorithm and program (Table A1) were designed for the λ',γ' diagram, and the Cartesian co-ordinates (λ',γ') of each of the lines are computed and plotted on a three-circle diagram (Fig. A1). L1, L2, L3 are λ_1', λ_2', λ_3', respectively. However, the Mohr loci plotted in Fig. A1 are equally applicable to other Mohr diagrams such as the polar stretch diagrams. So in the present paper, L1, L2, L3 will be equivalent to S_1', S_2', S_3'. In the (non-reciprocal) stretch diagram they would be S_3, S_2, S_1, respectively.

The section plane is defined in terms of its strike angle (S) and dip angle (D) measured with respect to λ_1' or S_1 vertical. λ_2' or S_2 N–S, and λ_3' or S_3 E–W, which is the orientation convention used throughout this paper (e.g. Fig. 3a). The plane can be considered as an array of lines, each of which must be perpendicular to P, the pole of the plane. Writing l, m, n as the direction cosines of P, and L, M, N for the direction cosines of any line lying in the plane, the following expressions can be written:

$$l = \cos \mathrm{D}$$
$$m = \sin \mathrm{S} \sin \mathrm{D}$$
$$n = (\sin^2 \mathrm{D} \cos^2 \mathrm{S})^{1/2}$$
$$L = \cos \phi_1'$$
$$M = \cos \phi_2'$$
$$N^2 = 1 - L^2 - M^2$$

and for mutual perpendicularity

$$lL + mM + nN = 0.$$

For each plane, 101 lines have been used, stepping ϕ_1' in 50 increments each side of the line of dip ($\phi'_{1\min} = 90 - \mathrm{D}°$) to the line of strike ($\phi'_{1\max} = 90°$). For the successive L values, M and N can be derived using the above equations (Table A1, lines 200–210, 220–222). The λ',γ' co-ordinates (LP, GP) are then computed (lines 212–214, 224–226) for L1, L2, L3 and L, M, N, using the standard formulae (Nadai 1950, p. 128). Each λ',γ' co-ordinate is successively plotted on a λ',γ' graph, and the principal semi-circles drawn, finally.

As already stated, these plots can be used for any topologically equivalent Mohr diagram (e.g. λ', S', S, $\dot{e}$), and L1, L2, L3 will refer to the appropriate principal axial values. The present program (Table A1) required L3 ≥ L2 ≥ L1 because L3 is the chosen dimension of the abscissa; it sets L1 = 1/(L2 × L3), and so is restricted to isochoric deformations. With simple changes, the program could be tailored to other more general uses.

Table A1. Program listing of a Basic program for plotting Mohr loci, using an IBM-compatible computer and HP-GL plotter language. Input is L3, L2, strike and dip. See Appendix text for explanation

```
10 REM mohr loci
15 OPEN "com1:9600,n,7,1,rs,cs65535,ds,cd" AS#1
20 CLS:PRINT TAB(13),"Mohr loci calculations and plot":PRINT
40 INPUT "enter value of L3";L3
50 INPUT "enter value of L2";L2
60 L1=1/(L2*L3)
100 INPUT "STRIKE =";STRIKE
110 INPUT "DIP=";DIP
115 GOSUB 1000
120 PI=3.14159
122 S=STRIKE*PI/180
124 D=DIP*PI/180
126 SS=SIN(S)
128 CS=COS(S)
130 SD=SIN(D)
132 CD=COS(D)
150 PHMIN=90-DIP
160 NT=DIP/50
170 FOR PH=PHMIN TO 90 STEP NT
174   RL=PH*PI/180
180   L=COS(RL)
190   RT=SQR(SD^2-L^2+.00001)
200   M=(-L*SS*CD+CS*RT)/SD
210   N=(-L*CD*CS-SS*RT)/SD
212   LP=L1*L^2+L2*M^2+L3*N^2
214   GP=SQR((L1-L2)^2*L^2*M^2+(L2-L3)^2*M^2*N^2+(L3-L1)^2*N^2*L^2)
216   GOSUB 2000
220   M=(-L*SS*CD-CS*RT)/SD
222   N=(-L*CD*CS+SS*RT)/SD
224   LP=L1*L^2+L2*M^2+L3*N^2
226   GP=SQR((L1-L2)^2*L^2*M^2+(L2-L3)^2*M^2*N^2+(L3-L1)^2*N^2*L^2)
230   GOSUB 2000
240 NEXT
260 PRINT#1,"sm;"
280 REM plot arcs
300 A=L2:B=L1
310 GOSUB 3000
320 A=L3:B=L1
330 GOSUB 3000
340 A=L3:B=L2
350 GOSUB 3000
410 INPUT "another plot ";RESP$
420 IF (RESP$="y" OR RESP$="Y")THEN PRINT #1,"pg;":GOTO 20
430 PRINT #1,"nr;sp0;"
490 CLOSE (1)
500 END
1000 REM initialise
1012 TITLE1$="L1="+STR$(L1)+"  L2="+STR$(L2)+"  L3="+STR$(L3)
1014 TITLE2$="strike="+STR$(STRIKE)+"  dip="+STR$(DIP)
1020 SFACTOR=6000/L3
1022 XSTART=500
1024 YSTART=500
1030 PRINT#1,"in;sp1;pa 6500,500;pd 500,500;pa 500,3500;"
1031 PRINT#1,"vs 10;fs 6;"
1034 PRINT#1,"sr 0.5,1;"
1040 FOR LOOP=0 TO L3+.1 STEP L3/10
1050   XP=LOOP*SFACTOR+XSTART
1060   YP=YSTART
1070   PRINT#1,"pu"XP,YP";pd"XP,YP-80";"
1080   PRINT#1,"pu"XP-50,YP-150";lb"LOOP CHR$(3)
1090 NEXT
1100 FOR LOOP=0 TO L3/2 STEP L3/10
1110  XP=XSTART
1120  YP=LOOP*SFACTOR+YSTART
1130  PRINT#1,"pu"XP,YP";pd"XP-80,YP";"
1140  PRINT#1,"pu"XP-350,YP+40";lb"LOOP CHR$(3)
1150 NEXT
1160 PRINT#1,"pu 1100,4000;sr;lb"TITLE1$ CHR$(3)
1170 PRINT#1,"pu 1100,3800;lb"TITLE2$ CHR$(3)
1174 PRINT#1,"sm.;"
1180 RETURN
2000 REM plot points
2010 XP=XSTART+LP*SFACTOR
2020 YP=YSTART+GP*SFACTOR
2030 PRINT#1,"pa"XP,YP";"
2040 RETURN
3000 REM plot arcs
3010 XCEN=(A+B)/2
3020 RAD=(A-B)/2
3030 XARCSTART=XSTART+(XCEN-RAD)*SFACTOR
3035 XCEN=XCEN*SFACTOR+XSTART
3040 PRINT#1,"pa"XARCSTART,YSTART";"
3050 PRINT#1,"pd;aa"XCEN,YSTART,"-180;"
3060 RETURN
```

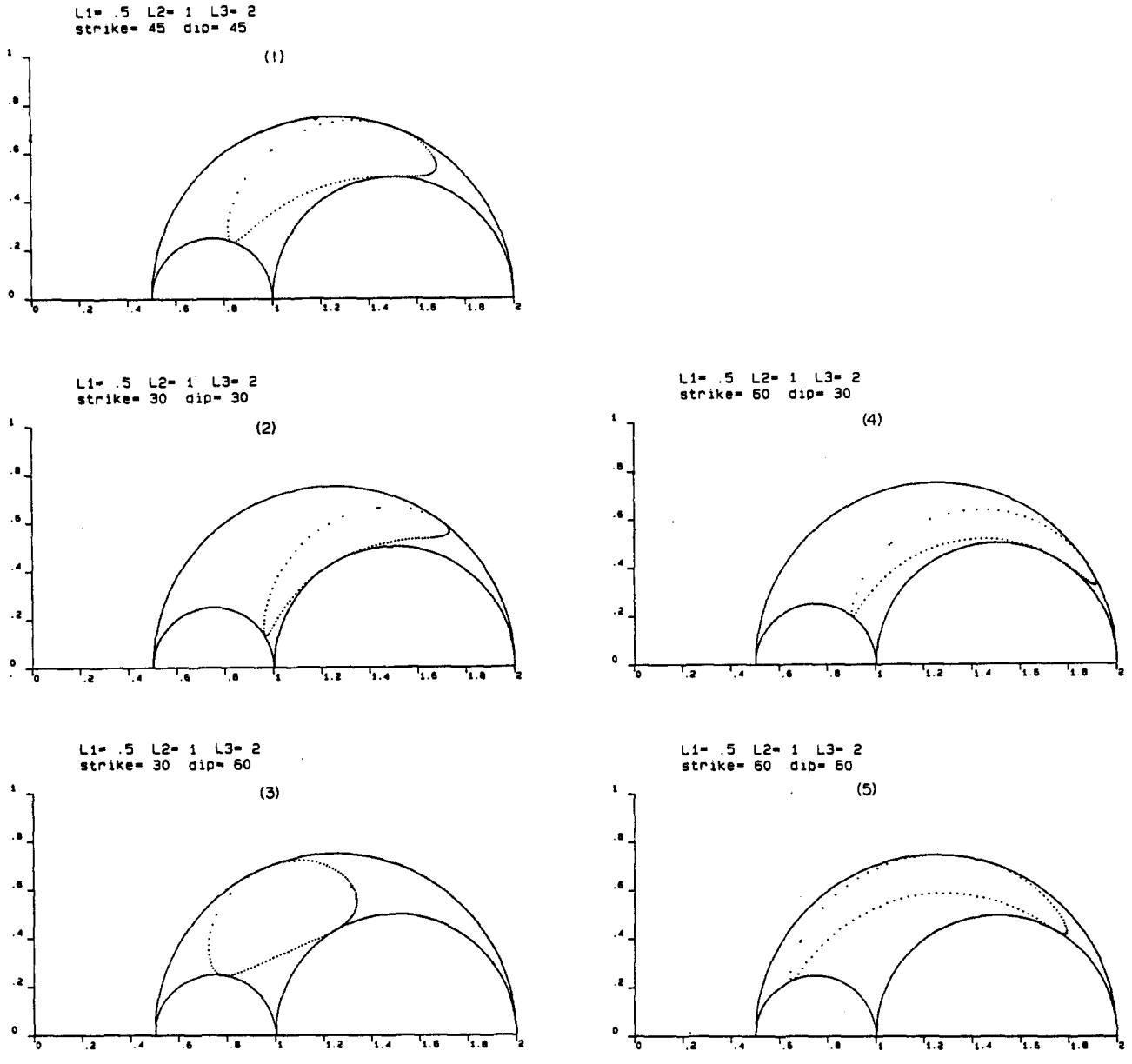

Fig. A1. Computer-plotted examples of type-3 Mohr loci. The method and all definitions are given in the Appendix.